

# Cross Quality Distillation

Jong-Chyi Su, Subhansu Maji

University of Massachusetts, Amherst  
{jcsu,smaji}@cs.umass.edu

**Abstract.** We propose a technique for training recognition models when high-quality data is available at training time but not at testing time. Our approach, called *Cross Quality Distillation (CQD)*, first trains a model on the high-quality data and encourages a second model trained on the low-quality data to generalize in the same way as the first. The technique is fairly general and only requires the ability to generate low-quality data from the high-quality data. We apply this to learn models for recognizing low-resolution images using labeled high-resolution images, non-localized objects using labeled localized objects, edge images using labeled color images, etc. Experiments on various fine-grained recognition datasets demonstrate that the technique leads to large improvements in recognition accuracy on the low-quality data. We also establish connections of CQD to other areas of machine learning such as domain adaptation, model compression, and learning using privileged information, and show that the technique is general and can be applied to other settings. Finally, we present further insights into why the technique works through visualizations and establishing its relationship to curriculum learning.

## 1 Introduction

One of the challenges in computer vision is to build models for recognition that are robust to various forms of degradation of the quality of the signal such as loss in resolution, lower signal-to-noise ratio, poor alignment, etc. For example, the performance of existing models for fine-grained recognition drop rapidly when the resolution of the input image is reduced (see Table 1). While it is natural to expect a drop in accuracy since it may be impossible to infer certain visual properties from the low-quality data, we are interested in models whose performance degrades more gracefully as the signal degrades. Such systems will have a significant impact in a wide range of applications including those where poor quality data poses critical challenges such as surveillance, recognition of satellite imagery, face recognition for biometrics, etc. To this end we propose a technique called *Cross Quality Distillation (CQD)* which utilizes the fact that in many scenarios abundant high-quality labeled data is available from which it is easy to automatically generate low-quality labeled data. However, instead of directly training a model on the low-quality data, which does not generalize well, we use the model trained on the high-quality data to guide the learning of a model on the low-quality by forcing agreement between their predictions on each example (Figure 1). This guidance helps the second model generalize

better on the low-quality data even though it does not have a direct access to the high-quality data at training or testing time.

We show experiments on training Convolutional Neural Network (CNN) models for recognizing fine-grained categories of birds and cars in images of non-localized objects using localized ones (Figure 3a), low-resolution images using high-resolution images (Figure 3b), line drawings using color images (Figure 3c), and distorted images using non-distorted images (Figure 3d). This is a challenging task even on the high-quality images, but performance of the models is often dramatically lower when applied on the low-quality images. Our experiments show that CQD leads to significant improvements over a model trained on the low-quality data and other strong baselines for domain adaptation. The model works across a variety of tasks and domains without any task-specific customization. We also present preliminary experiments to address the case when the quality of the test data varies across examples, e.g. differing resolutions, using mixture models that lead to further gains.

We also relate CQD to existing approaches in the literature, spanning areas of domain adaptation, model compression [1,2,3], and learning using privileged information [4]. Our technique can be seen as a simple generalization of the model compression approach pioneered by Bucilă et al. [1], and revived recently in the context of CNNs by Hinton et al. [2] and Ba and Caruana [3]. In model compression, the goal is to learn a simple classifier that can imitate a more complex classifier on the same input, whereas in CQD the two functions operate on different inputs. However, the ideas are complementary and can be combined. For example, we can use a deeper CNN trained on high-quality images to guide the learning of a shallower CNN on the low-quality images leading to even better generalization. Finally, we present insights into why the method works by relating it to the area of curriculum learning [5] and through visualizations of the learned models.

## 1.1 CQD framework

Assume that we have data in the form of  $(\mathbf{x}_i, \mathbf{z}_i, y_i)$ ,  $i = 1, 2, \dots, n$  where  $\mathbf{x}_i \in \mathcal{A}$  is the high-quality data,  $\mathbf{z}_i \in \mathcal{B}$  is the corresponding low-quality data, and  $y_i \in \mathcal{Y}$  is the target label. In practice only the high-quality data  $\mathbf{x}_i$  is needed since  $\mathbf{z}_i$  can be generated from  $\mathbf{x}_i$ . The idea of CQD is to first train a model  $f$  to predict the labels on the high-quality data and train a second model  $g$  on the low-quality data by forcing an agreement between their corresponding predictions by optimizing:

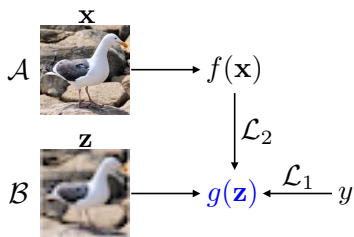


Fig. 1. The CQD framework.

$$g \leftarrow \arg \min_g \sum_{i=1}^n \mathcal{L}_1(g(\mathbf{z}_i), y_i) + \lambda \sum_{i=1}^n \mathcal{L}_2(g(\mathbf{z}_i), f(\mathbf{x}_i)) + \mathcal{R}(g). \quad (1)$$

Here,  $\mathcal{L}_1$  and  $\mathcal{L}_2$  are loss functions,  $\lambda$  is a trade-off parameter, and  $\mathcal{R}(g)$  is a regularization term. Since  $f$  trained and evaluated on the high-quality data generalizes better (i.e., has higher test accuracy) than  $g$  trained and evaluated on the low-quality data, by trying to imitate  $f$ ,  $g$  can learn to generalize better.

All our experiments are on multiclass classification and we model both  $f$  and  $g$  using CNNs with a final softmax layer to produce class probabilities  $\mathbf{p} = \sigma(\mathbf{z})$ , i.e.  $p_k = e^{z_k} / \sum_j e^{z_j}$ . We use the cross-entropy loss  $\mathcal{L}_1(\mathbf{p}, \mathbf{q}) = \sum_i q_i \log p_i$ , and the cross-entropy of the predictions scaled by a temperature parameter  $T$  for  $\mathcal{L}_2(\mathbf{p}, \mathbf{q}) = \mathcal{L}_1(\sigma(\log(\mathbf{p})/T), \sigma(\log(\mathbf{q})/T))$ . When  $T = 1$ , this reduces to the standard cross-entropy loss, but higher values of  $T$  lead to smoothed output probabilities. We also found that squared-error between the logits ( $\mathbf{z}$ ) worked similarly (see experiments for details).

## 1.2 Related work

Figure 2 illustrates the relationship of CQD to various techniques in the literature. The proposed optimization is inspired by the “knowledge distillation” approach of Hinton et al. [2] where they train a simple classifier, e.g. a shallow neural network, to imitate the outputs (or “soft targets”) of a complex classifier, e.g. deep neural network. Their experiments show that the simple classifier generalizes better when provided with the outputs of the complex classifier during training. This is based on an idea pioneered by Bucilă et al. [1] in a technique called “model compression” where simple classifiers are trained to match the predictions obtained from an ensemble of classifiers, leading to compact models. However, in this setting both the classifiers  $f$  and  $g$  operate on the same input, i.e.  $\mathbf{x}_i = \mathbf{z}_i$  in Equation 1 (Figure 2a). Hence, CQD can be seen as a generalization of model compression when  $\mathcal{A}$  and  $\mathcal{B}$  are different (Figure 2d).

Our work is related to the area of learning using privileged information (LUPI) [4] (Figure 2b). This framework deals with the case when additional information is available at training time but not at testing time. The general idea is to use the side information to guide the training of the models. For example, the SVM+ approach of Vapnik et al. [4] modifies the margin for each training example using the side information to facilitate the training on the input features. Most of these approaches require an explicit representation of the side information, i.e., the domain  $\mathcal{A}$  can be written as a combination of domain  $\mathcal{B}$  and side information domain  $\mathcal{S}$ . For example, such models have been used to learn classifiers on images when additional information about them such as tags and attributes are available at training time. Our approach is more general as it does not require an explicit representation of the side information and only requires that domain  $\mathcal{A}$  be more useful for predicting the target labels than  $\mathcal{B}$ . Through distillation of a model trained on domain  $\mathcal{A}$  to a model on domain  $\mathcal{B}$ , one can implicitly learn to use the side information.

Our work is also related to the area of domain adaptation which addresses the problem that the distribution of features is different during training and testing, leading to degradation in performance. For example, visual classifiers trained on clutter-free images of cars do not generalize well when applied to real-world

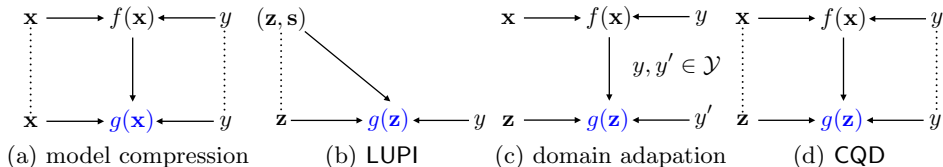


**Fig. 2.** Illustration of the relationships between CQD and other techniques. An arrow points to the direction of dependency between the variables, and dotted lines denote that the variables are observed together. For example, in model compression (panel a),  $g$  is trained to mimic the outputs of  $f$  on the same input  $\mathbf{x}$ . In LUPI, the  $g$  is trained with side information  $\mathbf{s}$  observed together with input  $\mathbf{z}$  (panel b). In domain adaptation,  $\mathbf{x}$  and  $\mathbf{z}$  are drawn independently from different domains but the tasks are the same, i.e.  $y, y' \in \mathcal{Y}$  (panel c). CQD can be seen as (i) a generalization of model compression where we allow the inputs of the two functions to be different (panel d), (ii) a specialization of domain adaptation when  $\mathbf{z}$  can be synthesized from  $\mathbf{x}$  and the corresponding labels are the same, and (iii) a technique for LUPI since by distilling the model  $f(\mathbf{z}, \mathbf{s})$  to  $g(\mathbf{z})$  we are learning to use the privileged information implicitly.

images of cars. Typically it is assumed that a large number of labeled examples exist for the source domain, but limited to no labeled data is available for the target domain. A number of techniques in computer vision address this problem by learning domain invariant representations. For example, the approach of “deep domain confusion” [6] learns a shared CNN to extract image features for two domains in a way that it is impossible to tell which domain the feature came from. A similar idea was explored in the work of Ganin and Lempitsky [7] where domain invariant features are learned by competing with an adversarial network trained to discriminate the domains. Other approaches learn a parametric transformation to align the representations of the two domains [8,9,10,11].

When some labeled data is available for the target domain (supervised case), methods for multi-task learning [12] are also applicable, including ones that are “frustratingly easy” [13]. CQD is a special case of supervised domain adaptation where we have correspondence between samples from the source and target domain. In other words, in supervised domain adaptation we have training data of the form  $(\mathbf{x}_i, y_i), \mathbf{x}_i \in \mathcal{A}$  and  $(\mathbf{z}_j, y_j), \mathbf{z}_j \in \mathcal{B}$ , where  $\mathbf{x}_i$  and  $\mathbf{z}_j$  are drawn independently from the source and target domain respectively, and  $y_i, y_j \in \mathcal{Y}$ . In CQD we know that  $\mathbf{x}_i$  and  $\mathbf{z}_i$  are two views of the same instance which allows richer constraints to adapt models across domains through distillation (Figure 2d). Our experiments show that distillation leads to greater improvements in accuracy compared to fine-tuning, a commonly used approach for domain adaptation. The idea of transferring task knowledge through distillation has been recently applied for simultaneous domain adaptation and task transfer by Tzeng et al. [14]. Their work proposes to match the average predicted label scores across examples in source domain to that of the target domain as instances lack one-to-one correspondence. In contrast, paired data in CQD allows matching of label distributions on a per-example basis, which is more powerful.

Although in our experiments quality refers to aspects of the data as resolution, alignment, and color, the notion is general and can be applied to other settings. For example, we use this technique to train a model to recognize distorted images of birds by distilling a model trained on non-distorted ones. Another application is where multiple sensors are simultaneously available. For example, labeled color plus depth data obtained from a RGB-D sensor can be used to learn a better model for RGB data. However, the lack of large labeled RGB-D datasets compared to RGB datasets makes CQD less attractive for this particular problem. Current methods use unlabeled RGB-D datasets to learn better representations of depth [15,16] and color [17] using unsupervised techniques. However, in the future as more accurate and novel sensing modalities become available and labeled datasets are collected for these modalities, CQD allows a systematic way of training better models for the legacy low-quality data.

## 2 Experiments

We begin by describing various datasets, CNN models, and training protocols used in our experiments. Section 2.1 describes the results of various experiments on cross quality distillation. Section 2.2 describes experiments for simultaneous quality distillation and model compression. Section 2.3 describes a simple strategy for classification when the quality of examples in the test set is unknown and varies by combining multiple models. Finally, Section 3 visualizes the distilled models to provide an intuition of why and how distillation works.

**Datasets** We perform experiments on the CUB 200-2011 dataset [18] consisting of 11,788 images of 200 different bird species, and on the Stanford cars dataset [19] consisting of 16,185 images of 196 cars of different models and makes. Classification requires the ability to recognize fine-grained details which are likely to be impacted when the quality of the images is poor. Using the provided images and bounding-box annotations in these datasets, we create several cross-quality datasets which are described in detail in the Section 2.1 and visualized in Figure 3. We use the training and test splits provided in the datasets.

**Models** In our experiments  $f$  and  $g$  are based on standard CNNs trained on the ImageNet dataset [20]. In particular we use the off-the-shelf vgg-m [21] and vgg-vd models [22] which obtain competitive performance on the ImageNet dataset. These are not the best performing models on the fine-grained recognition datasets, where multiple methods report results using novel model architectures [23,24,25,26], using additional annotations to train part and object detectors [27,28,29,30], etc. However, we believe that our method is general and can be applied to other recognition architectures as well.

**Methods** Below we describe various methods used in our experiments:

1. **Train on A:** Starting from the ImageNet pre-trained model, we replace the 1000-way classifier (last layer) of the model with a k-way classifier initialized

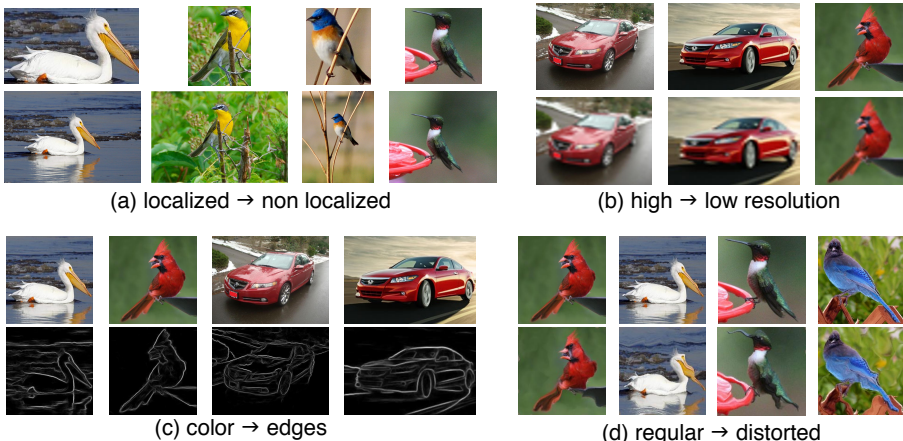


**Fig. 3.** Examples images from various cross-quality datasets used in our experiments. Images are from the birds [18] and cars dataset [19]. In each panel, the top row shows examples of the high-quality images and the bottom row shows examples of the corresponding low-quality images. These include (a) localized and non-localized images, (b) high- and low-resolution images, (c) color and edge images, and (d) regular and distorted images.

randomly and then fine-tune the entire model with a small learning rate on domain  $\mathcal{A}$ . This is a standard way of transfer learning using deep models, and has been successfully applied for a number of vision tasks including object detection, scene classification, semantic segmentation, texture recognition, and fine-grained classification [31,32,33,34,35,36,23].

2. **Train on  $\mathcal{B}$ :** This is identical to the earlier method except we fine-tune the ImageNet pre-trained model on domain  $\mathcal{B}$ .
3. **Train on  $\mathcal{A}$ , then train on  $\mathcal{B}$ :** This is a combination of the earlier two steps where the fine-tuning on domain  $\mathcal{B}$  is initialized from the model fine-tuned on domain  $\mathcal{A}$ . This can only be applied when both  $f$  and  $g$  have the same structure, e.g. identical CNN architectures. This is denoted by  $\mathcal{A}, \mathcal{B}$  in our experiments.
4. **Cross quality distillation:** Here we use a model  $f$  trained on domain  $\mathcal{A}$  (Method 1) to guide the learning of a second model  $g$  on domain  $\mathcal{B}$  using CQD (Equation 1). Like before, when  $f$  and  $g$  have identical structure we can initialize  $g$  from  $f$  instead of the ImageNet model with random weights for the last layer. We refer to this method as  $\mathcal{A}, \text{CQD}$  in our results.

**Optimization details** There are two parameters,  $T$  and  $\lambda$ , in the CQD model.  $T$  is the temperature parameter used to smooth the output probabilities (Equation 1). We tried  $T = \{1, 2, 5, 10\}$  on the validation set and found  $T = 10$  to be nearly optimal on all experiments. The optimal value of the trade-off parameter  $\lambda$  was found to be  $\lambda = 200$  for the CUB dataset and  $\lambda = 50$  for the CARS dataset. The optimization in Equation 1 was solved using batch stochastic

Method	Test	Localization	Resolution		Edge		Distortion
		CUB	CUB	CARS	CUB	CARS	CUB
$\mathcal{A}$	$\mathcal{A}$	67.3	67.3	58.8	67.3	58.8	67.3
$\mathcal{A}$	$\mathcal{B}$	57.0	41.0	7.6	1.8	4.6	50.0
$\mathcal{B}$	$\mathcal{B}$	60.2	60.7	41.1	29.0	44.4	59.3
$\mathcal{A}, \mathcal{B}$	$\mathcal{B}$	62.1	62.3	48.6	31.0	49.9	60.9
CQD	$\mathcal{B}$	63.4	63.4	46.2	32.7	48.7	62.8
$\mathcal{A}, \text{CQD}$	$\mathcal{B}$	<b>64.0</b>	<b>64.3</b>	<b>48.9</b>	<b>34.1</b>	<b>50.8</b>	<b>63.3</b>

**Table 1. Cross quality distillation results.** Per-image accuracy on birds dataset (CUB) [18] and Stanford cars dataset (CARS) [19] for various methods and quality losses. All results are using  $f = g = \text{vgg-m}$  model. The top row, i.e. train on  $\mathcal{A}$  and test on  $\mathcal{A}$ , is the upper bound of the performance in each setting. Training on  $\mathcal{A}$  and testing on  $\mathcal{B}$  often leads to a dramatic loss in performance (CARS high- to low-resolution drop is noteworthy). The proposed CQD technique outperforms the domain adaptation  $\mathcal{A}, \mathcal{B}$ , and significantly improves over  $\mathcal{B}$  baseline on all experiments.

gradient descent with momentum and weight decay. We use learning rate starting from 0.001 changing linearly to 0.00005 after 30 epochs. Other parameters are as follows: momentum=0.9, weight decay=0.0005, batch size=128 (=32 when training vgg-*vd*). Instead of cross-entropy on smoothed predictions, we also tried squared-distance on the logits  $\mathbf{z}$  as the loss function, as suggested by Ba et al. [3]. We found no significant difference between the two and used cross-entropy loss for all our experiments. Our implementation is based on MatConvNet [37].

## 2.1 Cross quality distillation results

We experiment with four different kinds of quality reduction to test the versatility of the approach. For each case we report per-image accuracy on the test set provided in the dataset. Results using the vgg-*m* model for both function  $f$  and  $g$  are summarized in Table 1 and are described in detail below. The main conclusions are summarized in the end of this section.

**Localized to non-localized distillation** To create the high-quality data, we use the provided bounding-boxes in the CUB dataset to crop the object in each image. In this dataset, birds appear in various locations and scales and in clutter. Hence, the localized images provide better quality data for training the models. This is reflected by the fact that the vgg-*m* trained and evaluated on the localized data obtains 67.3% accuracy, but when applied the non-localized data obtains only 57.0% accuracy (Table 1). When the model is trained on the non-localized data the performance improves to 60.2%. The sequential training baseline  $\mathcal{A}, \mathcal{B}$  improves the performance to 62.1%. CQD improves the results further to 64.0%.

For this task another baseline would be to train an object detector which first localizes the objects in images. For example, Krause et al. [38] report around 2.6% drop in accuracy (67.9%  $\rightarrow$  65.3%) when a R-CNN based object detector

is used to estimate bounding-boxes of objects at test time instead of using true bounding-boxes (Table 2 in [38], CNN+GT BBox+ft vs. R-CNN+ft). Remarkably, using CQD we observe only a 3.3% drop in performance (67.3%  $\rightarrow$  64.0%) without running any object detectors. Moreover, our method only requires a single CNN evaluation and hence is faster. In Section 3 we provide insights into why the distilled model performs better on non-localized images.

We did not report results on CARS on this setting since cars are fairly large and well-localized in images, and the performance difference between models trained on localized and non-localized images is small.

**High to low resolution distillation** Here we evaluate how models perform on images of various resolutions. For the CUB dataset we use the localized images resized to  $224 \times 224$  for the high-resolution images, downsample to  $50 \times 50$ , and upsample to  $224 \times 224$  again. For the CARS dataset we do the same for the entire image (bounding-boxes are not used).

The domain shift leads to large loss in performance here. On CUB the performance of the model trained on high-resolution data goes down from 67.3% to 41.0%, while the performance loss on cars is even more dramatic going from 58.8% to a mere 7.6%. Man-made objects like cars contain high-frequency details such as brand logos, shapes of head-lights, etc., which are hard to distinguish in the low-resolution images. A model trained on the low-resolution images does much better, achieving 60.7% and 41.1% accuracy on birds and cars respectively. Color cues in the low-resolution are much more useful for distinguishing birds than cars which might explain the better performance on birds. Using CQD the performance improves further to 64.3% and 48.9% on the low-resolution data. On CARS the effect of both sequential training and CQD is significant, leading to more than 7% boost in performance.

Unlike object bounding-boxes, it is hard to predict the high-resolution image from the low-resolution version. In the Appendix we show that techniques for super-resolution can be used to reduce the domain shift from high-resolution images, but do not bridge the gap completely. However, CQD and super-resolution are complementary and can be combined for additional benefits.

**Color to edges distillation** Recognizing line-drawings can be used for retrieval of images and 3D shapes using sketches and has several applications in search and retrieval. As a proxy for line-drawings, we test the performance of various methods on edge images obtained by running the edge detector of Dollár and Zitnick [39] on the color images of the localized birds, and cars dataset. In contrast to low-resolution images, edge images contain no color information but preserve most of the high-frequency details. This is reflected in the better performance of the model trained and evaluated on edge images on cars than birds (Table 1). The domain shift is large here, and a model trained on color images performs poorly on edge images, obtaining 1.8% and 4.6% accuracy on birds and cars respectively.

Using CQD, the performance improves significantly from 44.4% to 50.8% on cars. On the birds dataset the performance also improves from 29.0% to 34.1%. The strong improvements on recognizing line drawings using distillation suggests that a better strategy to recognize line drawings of shapes used in various sketch-based retrieval applications [40,41] is not to fine-tune models on edge images, but rather to first fine-tune the model on realistically rendered 3D models (e.g. with shading and texture) and then to distill the model to edge images.

**Non-distorted to distorted distillation** Here the high-quality dataset is the localized bird images. To distort an image, we use the thin plate spline transformation with uniform grid of  $14 \times 14$  control points. Each control point is mapped from a regular grid to a point randomly shifted by Gaussian distribution with 0 mean and 4 pixels variance. These produce distorted images as seen in Figure 4. More example pairs can be seen in Figure 3d. Recognizing these distorted images is challenging, and the performance of a model trained and evaluated on such images is 8% worse (67.3%  $\rightarrow$  59.3%). Using CQD the performance improves from 59.3% to 63.3%. This also improves over the  $\mathcal{A}, \mathcal{B}$  baseline by 2.4%.

On this dataset a baseline would be to remove the distortion by alignment methods such as congealing [42], or use a model that estimates deformations during learning, such as spatial transformer networks [26]. These methods are likely to work well but they require the knowledge of the space of transformations and are non-trivial to implement. On the other hand, CQD is able to nearly halve the drop in performance of the same CNN model without any knowledge of the nature of distortion and is easy to implement. Thus, CQD may be used whenever we can model the distortions algorithmically. For example, computer graphics techniques can be used to model the distortions caused due to imaging under water, through a glass covered in water drops, etc., to train recognition models without requiring additional labeling.

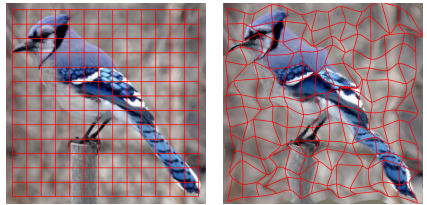


Fig. 4. Thin plate spline distortion.

**Summary** The main conclusions of the experiments are (see Table 1):

1. Some domain adaptation is necessary since the performance of models trained on high-quality data is poor on the low-quality data.
2. Sequential fine-tuning on the high-quality data followed by low-quality data ( $\mathcal{A}, \mathcal{B}$ ) works better than directly fine-tuning on the low-quality data ( $\mathcal{B}$ ). In Section 3 discuss the connections of this strategy to curriculum learning [5].
3. CQD improves the results further compared to  $\mathcal{A}, \mathcal{B}$  suggesting that distillation (when possible) provides better domain adaptation than fine-tuning.
4. CQD is robust and works with minor modifications, such as setting the values of  $T$  and  $\lambda$ , across a wide variety of quality losses. In most cases, CQD cuts the performance gap between the high- and low-quality data in half.

## 2.2 Simultaneous quality distillation and model compression

In this section we experiment if a deeper CNN trained on high-quality data can be distilled to a shallow CNN trained on the low-quality data. This is the most general version of CQD where both the domains and functions  $f, g$  change. The formulation in Equation 1 does not require  $f$  and  $g$  to be identical. However, the  $\mathcal{A}, \mathcal{B}$  baseline cannot be applied here.

We perform experiments on the CUB dataset using localized and non-localized images described earlier. The deeper CNN is the sixteen-layer “very deep” model (vgg-vd) and the shallow CNN is the five-layer vgg-m model used in the experiments so far. The optimal parameters obtained on the validation set for this setting were  $T = 10, \lambda = 50$ .

The results are shown in Table 2. The first row contains results using CQD for vgg-m model which are copied from Table 1 for ease of comparison. The third row shows the same results using the vgg-vd model. The accuracy is higher across all tasks. CQD leads to an improvement of 2.9% (69.5%  $\rightarrow$  72.4%) for the deeper model. The middle row shows results for training the vgg-m model on non-localized images from a vgg-vd model trained on the localized images. This leads to a further improvement of 1.2% (63.4%  $\rightarrow$  64.6%) suggesting that model compression and cross quality distillation can be seamlessly combined.

$f \rightarrow g$	Training $\rightarrow$ Testing		
	$\mathcal{A} \rightarrow \mathcal{A}$	$\mathcal{B} \rightarrow \mathcal{B}$	CQD $\rightarrow \mathcal{B}$
vgg-m $\rightarrow$ vgg-m	67.3	60.2	63.4
vgg-vd $\rightarrow$ vgg-m	-	-	64.6
vgg-vd $\rightarrow$ vgg-vd	74.9	69.5	72.4

**Table 2.** Accuracy of various techniques on the CUB localized/non-localized dataset.

## 2.3 Multi-resolution models

So far we showed that the accuracy of the model depends crucially on the match between the quality of the data it is trained and evaluated on. Models trained on high-resolution data do not generalize well on low-resolution data, and at the same time models that do well on low-resolution data are sub-optimal when evaluated on high-resolution data (Table 3). However, in reality most test sets contain data of varying degrees of resolution and a single model may not work well. But if we knew the quality of the test example ahead of time, we can apply the appropriate model.

Here we propose a simple solution to this problem where we train a classifier to predict the resolution of the data and apply the appropriate model. To predict the resolution, we compute the fast Fourier transform for each image to obtain the magnitude of frequency-domain response, resize it to  $65 \times 65$  as a way of

dimensionality reduction and take the logarithm of the values for numerical stability. Using these features we train a linear classifier to predict whether an image is high- or low-resolution (Figure 5). This is an easy task in this feature space, and our classifier is able to recognize if an image is high- or low-resolution with more than 99.5% accuracy on the CARS dataset.

We experiment with the CARS dataset and construct a test set by merging both the high and low resolution images denoted by “ $\mathcal{A} + \mathcal{B}$ ”. Another baseline would be to simply train on the  $\mathcal{A} + \mathcal{B}$  training set. We found that this performs at 52.0% when tested on  $\mathcal{A} + \mathcal{B}$ , beating both the model  $\mathcal{A}$  and  $\mathcal{A},\text{CQD}$  even though it does not beat these methods on  $\mathcal{A}$  or  $\mathcal{B}$  individually (Table 3). The performance of the oracle that knows the resolution of each test example and can pick the appropriate model performs at 53.9%. Our multi-resolution model which relies on the predictions of a resolution classifier performs nearly as well at 53.8%.

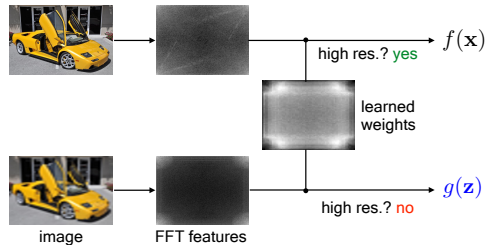


Fig. 5. Multi-resolution model.

Our experiments suggest that domain shifts observed due to changes in image quality remain a problem for existing CNN architectures. Systematically dealing with them, e.g. using multi-resolution models, can significantly improve the robustness of recognition systems.

Model	Test on $\mathcal{A}$	Test on $\mathcal{B}$	Test on $\mathcal{A} + \mathcal{B}$
$\mathcal{A}$	58.8	7.6	33.2
$\mathcal{A},\text{CQD}$	31.8	48.9	40.3
$\mathcal{A} + \mathcal{B}$	57.3	46.8	52.0
Multi-res	-	-	<b>53.8</b>
Oracle	58.8	48.9	53.9

Table 3. Classification accuracy on the multi-resolution car dataset. Our multi-resolution model consisting of a resolution classifier and two models, one for each resolution, improves performance by 1.8% over the baseline and performs nearly as well as the oracle classifier. See text for details.

### 3 Understanding why cross quality distillation works

In this section we analyze why CQD is an effective way of domain adaptation by drawing parallels from the area of curriculum learning and visualizing the regions within images used by the learned models to make predictions.

### 3.1 Connections to curriculum learning

Curriculum learning is the idea that learning algorithms generalize better when training examples are presented in the order of their difficulty. Bengio et al. [5] showed a variety of experiments where non-convex learners reach better optima when more difficult examples are introduced gradually. In one experiment a multi-layer neural network was trained to recognize shapes. There were two kinds of shapes: **BasicShapes** which are canonical circles, squares, and triangles, and **GeomShapes** which are affine distortions of the **BasicShapes** on more complex backgrounds. Even when the performance was evaluated on a test set consisting of only **GeomShapes**, the model which was first trained on the **BasicShapes** followed by training on **GeomShapes**, performed better than the model that was only trained on **GeomShapes**, or the one trained with a random ordering of both types of shapes.

We observe a similar phenomenon when training CNNs on the low-quality data. For example, on the CARS dataset, sequential training  $\mathcal{A}, \mathcal{B}$  outperforms the model trained on low-resolution data  $\mathcal{B}$ , as well as the model trained on the mixture of datasets  $\mathcal{A} + \mathcal{B}$ , when evaluated on the low-resolution data  $\mathcal{B}$  (48.6% vs. 41.1% vs. 46.8% respectively). Since low-quality data is generally difficult to recognize, introducing them gradually might explain the better performance of the sequential training. Additional benefits of CQD come from the fact that we have paired high- and low-quality images allowing better knowledge transfer through distillation.

### 3.2 Understanding CQD through gradient visualizations

Here we investigate how the knowledge transfer occurs between a model trained on localized images and non-localized images. Our intuition is that by trying to mimic the model trained on the localized images a model must learn to ignore the background clutter. In order to verify this intuition, we compute the gradient of log-likelihood of the true label of an image with respect to the image using both the CQD model and  $\mathcal{B}$  model. Note that both of these models are trained on non-localized images only. Figure 6-left shows the gradients for two different images. The darkness of each pixel  $i$  is proportional to the norm of the gradient vector at that pixel  $\|G_i\|_2$ ,  $G_i = [G_i^r, G_i^g, G_i^b]$  for each of the  $r, g, b$  color channels. The gradients of the CQD model are more contained within the bounding-box of the object, suggesting a better invariance to background clutter. As a further investigation we compute the fraction of gradients within the box:

$$\tau = \frac{\sum_{i \in \text{box}} \|G_i\|_2}{\sum_{i \in \text{image}} \|G_i\|_2}$$

This ratio is a measure of how localized the relevant features are within the bounding-box. A model based on a perfect object detector will have  $\tau = 1$ . We compute  $\tau$  for 1000 images for both CQD and  $\mathcal{B}$  models and visualize them on a scatter plot as seen in Figure 6-right. On average the distilled model has higher  $\tau$  than the non-distilled one, confirming our intuition that the distilled model is implicitly able to localize objects.

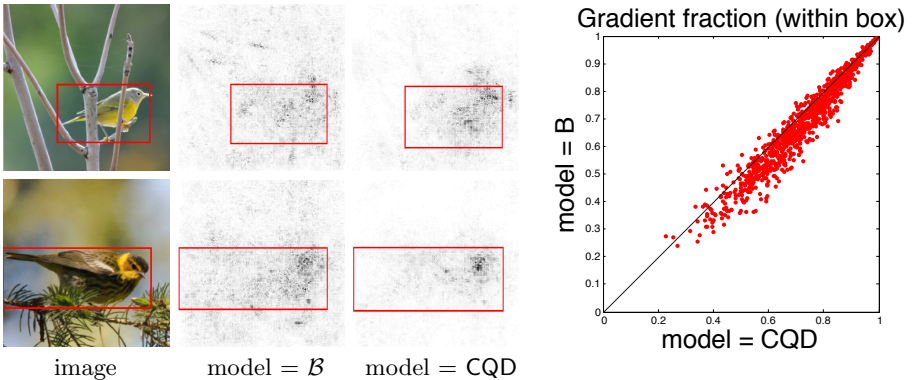


**Fig. 6. Left:** Image and gradient of the image with respect to the true class label for the model trained on  $\mathcal{B}$  (non-localized images) and CQD from a model trained on localized images. Darker pixels represent higher gradient value. The gradients of the model trained using CQD are more focused on the foreground object. **Right:** The scatter plot of the fraction of total gradient within the bounding-box for 1000 training images for the two models. On average CQD has more gradient energy inside the bounding-box.

### 3.3 Visualizing top confusions on low-resolution cars

Figure 8 shows the top five pairs of the classes that have the highest reduction in pairwise confusion going from  $\mathcal{B}$  model to  $\mathcal{A}, \text{CQD}$  model. The pairwise confusion is measured as  $c(i, j) + c(j, i)$ , where  $c(i, j)$  is the fraction of examples of class  $i$  classified as class  $j$  on the test set. These classes tend to be ones which are easily distinguished by the high-resolution model but are difficult to recognize in the low-resolution version.

## 4 Conclusion

We proposed a simple generalization of distillation, originally used for model compression, for cross quality model adaptation. We showed that CQD achieves superior performance than domain adaptation techniques such as fine-tuning on a range of tasks, including recognizing low-resolution images, non-localized images, edge images, and distorted images. Our experiments suggest that recognizing low-quality data is a challenge for existing methods, but by developing better techniques for domain adaptation one can significantly reduce the performance gap between the high- and low-quality data. We also presented mixture models for multi-resolution recognition that lead to further gains. We presented insights into why CQD works by relating it to various areas in machine learning and by visualizing the learned models.

One of the challenges in deep learning is to train models when limited training data is available for a task. A common strategy is to provide additional annotations to create intermediate tasks that can be easily solved. For example, annotations can be used to train part detectors to obtain pose, viewpoint, and



**Fig. 7.** Top five class pairs with the highest reduction in pairwise confusion going from the model trained on  $\mathcal{B}$  to one trained using  $\mathcal{A}, \mathcal{C}, \mathcal{QD}$  in the cars low resolution dataset.

location-invariant representations, making the fine-grained recognition problem easier. However, these require annotation-specific solutions and this strategy does not scale as new annotations become available. An alternate strategy is to use CQD by simply treating these annotations as additional features, learning a classifier in the combined space of images and annotations, and then distilling it to a model trained on images only. This strategy may be sub-optimal but is much more scalable and can be easily applied as new forms of side information, such as additional modalities and annotations, become available over time. In future work, we aim to develop strategies for distilling deep models trained from richly-annotated training data for better generalization from small training sets.

## Appendix

### A Using super-resolution for up-sampling

Here we present experiments for recognizing low resolution images using super-resolution (SR) algorithms. SR algorithms [43,44,45] rely on natural image statistics to better up-sample the image than bicubic interpolation used in our earlier experiments. We use the SR algorithm of Dong et al. [43] which is implemented as a three-layer CNN and was shown to outperform the previous state-of-the-art at the time of its publication. Their models implement various integer multiples of up-sampling up to a factor of four. Thus we apply their algorithm from the size  $56 \times 56$  to  $224 \times 224$ <sup>1</sup>. Note that the size we used for the low resolution

<sup>1</sup> We use the pre-trained 9-5-5(ImageNet)/x4 model provided by the authors.

baseline is  $50 \times 50$  providing a slight advantage to the SR baseline. Figure 8 and Figure 9 show images from CARS and CUB dataset respectively up-sampled using bicubic and the SR algorithm.

Table 4 shows the results of methods  $\mathcal{A}$ ,  $\mathcal{B}$  and  $\mathcal{A},\text{CQD}$  on the bicubic and SR upsampled images. On the CARS dataset the SR method provides a significant improvement where  $\mathcal{B}$ , i.e. a CNN fine-tuned on SR images evaluated on SR images is roughly 7% better ( $41.1\% \rightarrow 48.0\%$ ) than the same on bicubic interpolated images. CQD provides additional benefits improving the results to 53.5% getting close to the upper-bound of 58.8%. On the CUB dataset the gains are smaller as the results are closer to the upper bound of 67.3%. Overall, the CQD works slightly worse on the SR images compared to the bicubic interpolation (63.6% vs. 64.3%). However, in both cases SR reduces the domain shift from the high-resolution to low-resolution images as reflected by the fact that the  $\mathcal{A}$  method works much better on the SR images. These experiments suggest that in some cases SR and CQD are complementary and can be combined for additional benefits.

Dataset		Method			Upper Bound
		$\mathcal{A}$	$\mathcal{B}$	$\mathcal{A},\text{CQD}$	
CARS	Bicubic	7.6	41.1	48.9	58.8
	SR	19.3	48.0	53.5	
CUB	Bicubic	41.0	60.7	64.3	67.3
	SR	52.2	62.2	63.6	

**Table 4.** Effect of using super-resolution algorithms for up-sampling images.

## References

1. Bucilua, C., Caruana, R., Niculescu-Mizil, A.: Model compression. In: Proceedings of the 12th ACM SIGKDD International Conference on Knowledge Discovery and Data Mining, KDD. (2006) 2, 3
2. Hinton, G., Vinyals, O., Dean, J.: Distilling knowledge in a neural network. In: Deep Learning and Representation Learning Workshop, NIPS. (2014) 2, 3
3. Ba, J., Caruana, R.: Do deep nets really need to be deep? In: Advances in neural information processing systems. (2014) 2654–2662 2, 7
4. Vapnik, V., Vashist, A.: A new learning paradigm: Learning using privileged information. *Neural Networks* **22**(5) (2009) 544–557 2, 3
5. Bengio, Y., Louradour, J., Collobert, R., Weston, J.: Curriculum learning. In: Proceedings of the 26th annual international conference on machine learning, ACM (2009) 41–48 2, 9, 12
6. Tzeng, E., Hoffman, J., Zhang, N., Saenko, K., Darrell, T.: Deep domain confusion: Maximizing for domain invariance. arXiv preprint arXiv:1412.3474 (2014) 4
7. Ganin, Y., Lempitsky, V.: Unsupervised domain adaptation by backpropagation. arXiv preprint arXiv:1409.7495 (2014) 4

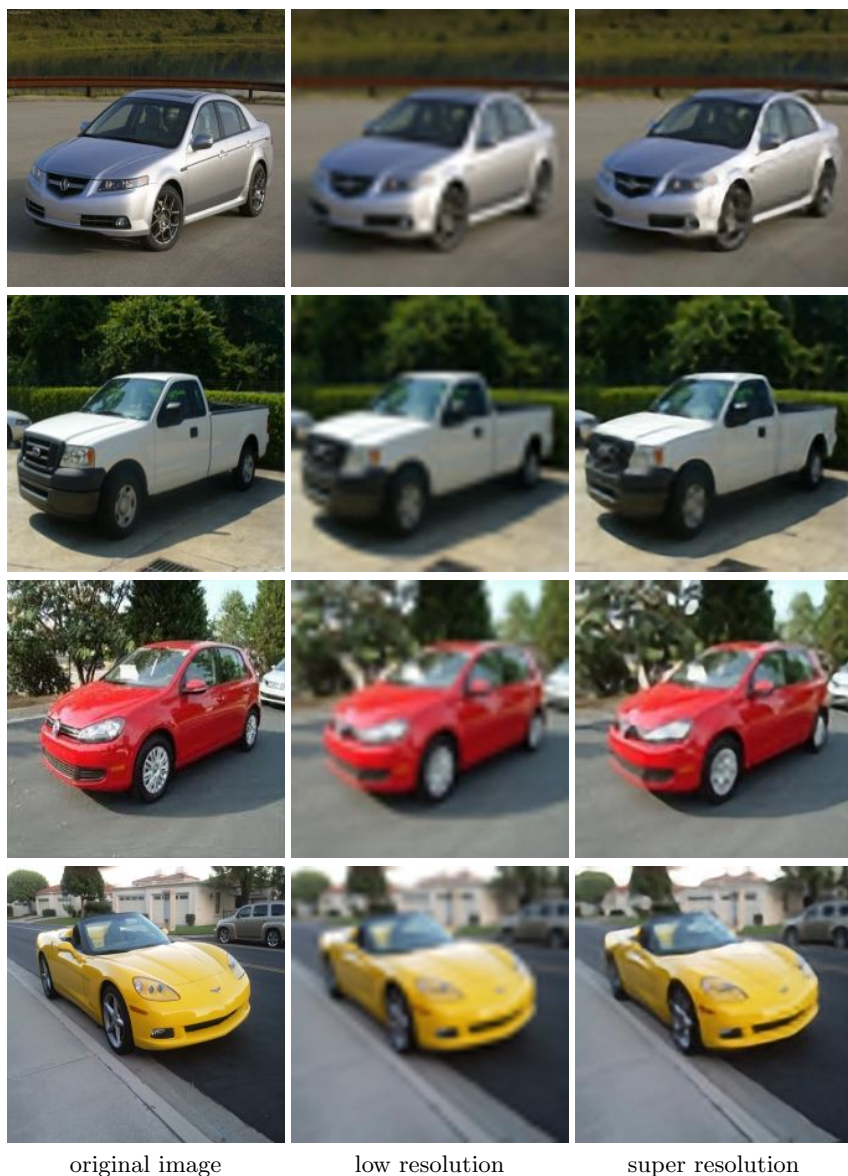
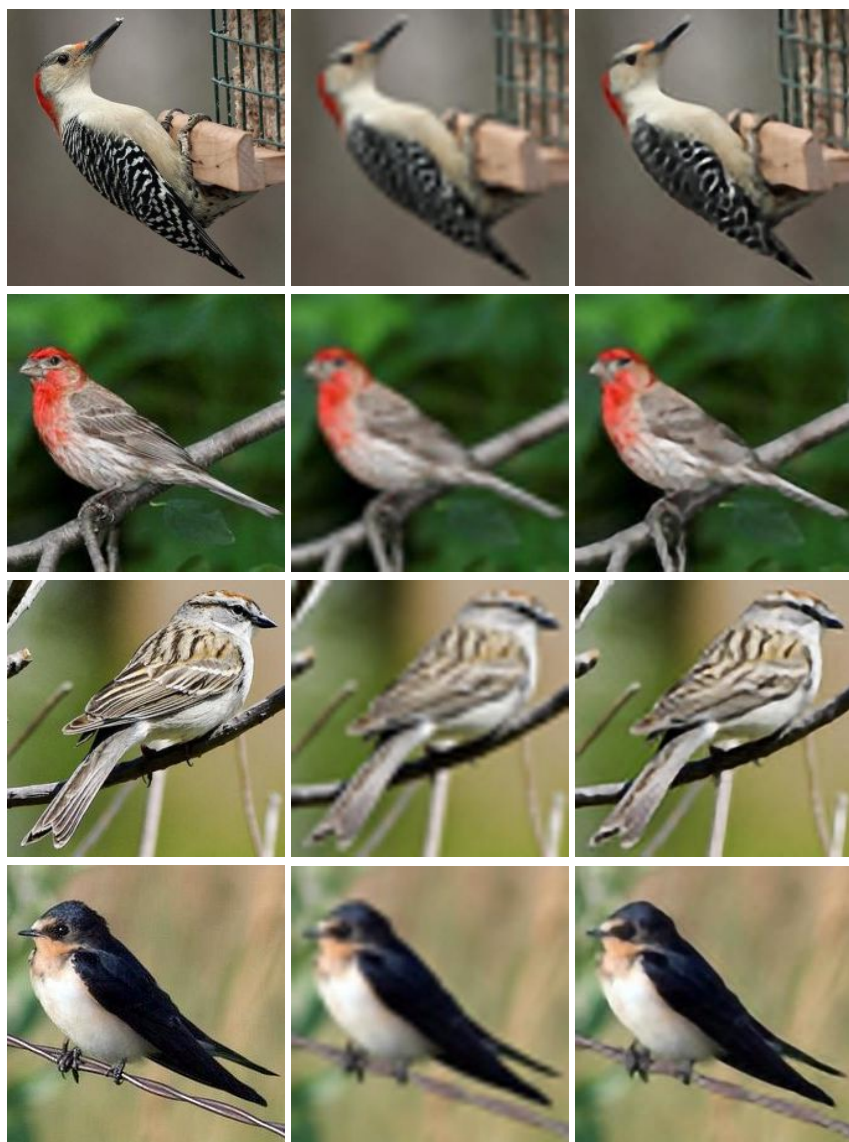


**Fig. 8.** Original images from the CARS dataset resized to  $224 \times 224$  (left column), upsampled from  $50 \times 50$  to  $224 \times 224$  using bicubic interpolation (middle column), and from  $56 \times 56$  to  $224 \times 224$  using SR algorithm [43] (right column).



original image

bicubic interpolation

super resolution

**Fig. 9.** Original images from the CUB dataset resized to  $224 \times 224$  (left column), upsampled from  $50 \times 50$  to  $224 \times 224$  using bicubic interpolation (middle column), and from  $56 \times 56$  to  $224 \times 224$  using SR algorithm [43] (right column).

8. Fernando, B., Habrard, A., Sebban, M., Tuytelaars, T.: Unsupervised visual domain adaptation using subspace alignment. In: Proceedings of the IEEE International Conference on Computer Vision. (2013) 2960–2967 [4](#)
9. Saenko, K., Kulis, B., Fritz, M., Darrell, T.: Adapting visual category models to new domains. In: Computer Vision–ECCV 2010. Springer (2010) 213–226 [4](#)
10. Sun, B., Feng, J., Saenko, K.: Return of frustratingly easy domain adaptation. arXiv preprint arXiv:1511.05547 (2015) [4](#)
11. Kulis, B., Saenko, K., Darrell, T.: What you saw is not what you get: Domain adaptation using asymmetric kernel transforms. In: Computer Vision and Pattern Recognition (CVPR), 2011 IEEE Conference on, IEEE (2011) 1785–1792 [4](#)
12. Caruana, R.: Multitask learning. *Machine learning* **28**(1) (1997) 41–75 [4](#)
13. Daumé III, H.: Frustratingly easy domain adaptation. *ACL 2007* (2007) 256 [4](#)
14. Tzeng, E., Hoffman, J., Darrell, T., Saenko, K.: Simultaneous deep transfer across domains and tasks. In: The IEEE International Conference on Computer Vision (ICCV). (December 2015) [4](#)
15. Gupta, S., Hoffman, J., Malik, J.: Cross modal distillation for supervision transfer. *CoRR abs/1507.00448* (2015) [5](#)
16. Hoffman, J., Gupta, S., Leong, J., Guadarrama, S., Darrell, T.: Cross-modal adaptation for rgb-d detection. In: International Conference in Robotics and Automation (ICRA). (2016) [5](#)
17. Chen, L., Li, W., Xu, D.: Recognizing rgb images by learning from rgb-d data. In: Proceedings of the IEEE Conference on Computer Vision and Pattern Recognition. (2014) 1418–1425 [5](#)
18. Wah, C., Branson, S., Welinder, P., Perona, P., Belongie, S.: The Caltech-UCSD Birds-200-2011 Dataset. Technical Report CNS-TR-2011-001, CalTech (2011) [5](#), [6](#), [7](#)
19. Krause, J., Stark, M., Deng, J., Fei-Fei, L.: 3d object representations for fine-grained categorization. In: Computer Vision Workshops (ICCVW), 2013 IEEE International Conference on. (2013) [5](#), [6](#), [7](#)
20. Deng, J., Dong, W., Socher, R., Li, L.J., Li, K., Fei-Fei, L.: ImageNet: A Large-Scale Hierarchical Image Database. In: CVPR. (2009) [5](#)
21. Chatfield, K., Simonyan, K., Vedaldi, A., Zisserman, A.: Return of the devil in the details: Delving deep into convolutional nets. In: British Machine Vision Conference (BMVC). (2014) [5](#)
22. Simonyan, K., Zisserman, A.: Very deep convolutional networks for large-scale image recognition. *CoRR abs/1409.1556* (2014) [5](#)
23. Lin, T.Y., RoyChowdhury, A., Maji, S.: Bilinear cnn models for fine-grained visual recognition. arXiv preprint arXiv:1504.07889 (2015) [5](#), [6](#)
24. Cimpoi, M., Maji, S., Vedaldi, A.: Deep filter banks for texture recognition and description. In: IEEE Conference on Computer Vision and Pattern Recognition (CVPR). (2015) [5](#)
25. Sermanet, P., Frome, A., Real, E.: Attention for fine-grained categorization. *CoRR abs/1412.7054* (2014) [5](#)
26. Jaderberg, M., Simonyan, K., Zisserman, A., et al.: Spatial transformer networks. In: Advances in Neural Information Processing Systems. (2015) 2008–2016 [5](#), [9](#)
27. Bourdev, L., Maji, S., Malik, J.: Describing People: Poselet-Based Approach to Attribute Classification. In: International Conference on Computer Vision (ICCV). (2011) [5](#)
28. Zhang, N., Donahue, J., Girshick, R., Darrell, T.: Part-based R-CNNs for fine-grained category detection. In: European Conference on Computer Vision (ECCV). (2014) [5](#)

29. Zhang, N., Paluri, M., Rantazo, M., Darrell, T., Bourdev, L.: Panda: Pose aligned networks for deep attribute modeling. In: IEEE Conference on Computer Vision and Pattern Recognition (CVPR). (2014) [5](#)
30. Branson, S., Horn, G.V., Belongie, S., Perona, P.: Bird species categorization using pose normalized deep convolutional nets. In: British Machine Vision Conference (BMVC). (2014) [5](#)
31. Donahue, J., Jia, Y., Vinyals, O., Hoffman, J., Zhang, N., Tzeng, E., Darrell, T.: Decaf: A deep convolutional activation feature for generic visual recognition. In: International Conference on Machine Learning. (2013) [6](#)
32. Razavin, A.S., Azizpour, H., Sullivan, J., Carlsson, S.: Cnn features off-the-shelf: An astounding baseline for recognition. In: DeepVision workshop. (2014) [6](#)
33. Girshick, R.B., Donahue, J., Darrell, T., Malik, J.: Rich feature hierarchies for accurate object detection and semantic segmentation. In: IEEE Conference on Computer Vision and Pattern Recognition (CVPR). (2014) [6](#)
34. Cimpoi, M., Maji, S., Kokkinos, I., Mohamed, S., Vedaldi, A.: Describing textures in the wild. In: IEEE Conference on Computer Vision and Pattern Recognition (CVPR). (2014) [6](#)
35. Long, J., Shelhamer, E., Darrell, T.: Fully convolutional networks for semantic segmentation. IEEE Conference on Computer Vision and Pattern Recognition (CVPR) (2015) [6](#)
36. Mostajabi, M., Yadollahpour, P., Shakhnarovich, G.: Feedforward semantic segmentation with zoom-out features. IEEE Conference on Computer Vision and Pattern Recognition (CVPR) (2015) [6](#)
37. Vedaldi, A., Lenc, K.: Matconvnet-convolutional neural networks for matlab. arXiv preprint arXiv:1412.4564 (2014) [7](#)
38. Krause, J., Jin, H., Yang, J., Fei-Fei, L.: Fine-grained recognition without part annotations. In: ICCV, International Conference on Computer Vision (2015) 5546–5555 [7](#), [8](#)
39. Dollár, P., Zitnick, C.L.: Structured forests for fast edge detection. In: ICCV, International Conference on Computer Vision (2013) [8](#)
40. Su, H., Maji, S., Kalogerakis, E., Learned-Miller, E.: Multi-view convolutional neural networks for 3d shape recognition. arXiv preprint arXiv:1505.00880 (2015) [9](#)
41. Wang, F., Kang, L., Li, Y.: Sketch-based 3d shape retrieval using convolutional neural networks. In: The IEEE Conference on Computer Vision and Pattern Recognition (CVPR). (2015) [9](#)
42. Huang, G., Mattar, M., Lee, H., Learned-Miller, E.G.: Learning to align from scratch. In: Advances in Neural Information Processing Systems. (2012) 764–772 [9](#)
43. Dong, C., Loy, C.C., He, K., Tang, X.: Learning a deep convolutional network for image super-resolution. In: Computer Vision–ECCV 2014. Springer (2014) 184–199 [14](#), [16](#), [17](#)
44. Huang, J.B., Singh, A., Ahuja, N.: Single image super-resolution from transformed self-exemplars. In: IEEE Conference on Computer Vision and Pattern Recognition. (2015) [14](#)
45. Timofte, R., De Smet, V., Van Gool, L.: A+: Adjusted anchored neighborhood regression for fast super-resolution. In: Computer Vision–ACCV 2014. Springer (2014) 111–126 [14](#)